JOURNAL OF COMPUTATIONAL PHYSICS 117, 350–363 (1995)

Several Symbolic Augmented Chebyshev Expansions for Solving the Equation of Radiative Transfer*

JAY I. FRANKEL

Mechanical and Aerospace Engineering Department, University of Tennessee, Knoxville, Knoxville, Tennessee 37996-2210

Received April 1, 1993; revised September 20, 1994

Three expansion methods are described using Chebyshev polynomials of the first kind for solving the integral form of the equation of radiative transfer in an isotropically scattering, absorbing, and emitting plane-parallel medium. With the aid of symbolic computation, the unknown expansion coefficients associated with this choice of basis functions are shown to permit analytic resolution. A unified and systematic solution treatment is offered using the projection methods of collocation, Ritz-Galerkin, and weighted-Galerkin. Numerical results are presented contrasting the three expansion methods and comparing them with existing benchmark results. New theoretical results are presented illustrating rigorous error bounds, residual characteristics, accuracy, and convergence rates.

1. INTRODUCTION

In radiative [1, 2] and neutron [3] transport theories, utilization of the equivalent integral form of the Boltzmann transport equation has often been called upon when considering highly anisotropic scattering in either a plane-parallel [4, 5] or spherical medium [6]. Peierl's equation produces (i) a reduction in dimensionality leading to a pure (smoothing) integral form, and (ii) a direct relation with several key physical quantities of interest [4, 5]. Unfortunately, the equivalent integral form also leads to a system of weakly singular Fredholm integral equations of the second kind. The appearance of the first exponential integral function, as a kernel function, introduces a logarithmic singularity as its argument vanishes.

Recently, Frankel [4] alluded to the natural implementation of symbolic computation to the integral form of the transport equation. Unfortunately, no symbolic implementation was actually performed. Indeed, only a crude numeric solution, based on singularity subtraction [7–9] and trapezoidal integration [10], was used. It is interesting to note that accurate results still resulted.

Owing to a lack of satisfactory closure on several fronts [4], this paper addresses three particular issues not previously resolved. In order to illustrate several fundamental points, this study focuses on radiative transport in an isotropically scattering plane-parallel medium. Extension to the general anisotropic scattering case will be evident. Thus, the purpose of the present exposition is threefold: (i) to develop three expansion methods which make use of Chebyshev polynomials of the first kind as the set of orthogonal basis functions; (ii) to implement and demonstrate the utility of symbolic computation, such as offered by the packages Mathematica® and Maple, for augmenting the solution methodology; and (iii) to present some informative residual/error and convergence analyses which are intended to indicate performance and accuracy of the methods.

This paper is divided into three major sections. In Section 2, we formulate the problem of interest. In Section 3, we introduce a series representation for the zeroth Legendre moment of the intensity and develop the three solution methods for finding the unknown expansion coefficients. In Section 4, we present results and discuss the merit of the proposed approach.

2. FORMULATION

In this section, we present the necessary formulation of the equations governing the zeroth Legendre moment of the radiative intensity in a plane-parallel, isotropically scattering, absorbing, and emitting medium. The transformation from the integrodifferential form of the equation of radiative transfer to the pure integral form can be found in the fine expositions by Ozisik [1] and Duderstadt and Martin [3].

2.1. *Peierl's Equation*

We begin by considering the integral form of the transport equation [1, 3, 4], namely,

$$G(\eta) = f^{\alpha}(\eta) + \frac{\lambda}{2}\int_{\xi=-1}^{1} K(\alpha|\eta-\xi|)G(\xi)\,d\xi, \quad \eta \in [-1, 1], \tag{2.1a}$$

where $G(\eta)$ is the zeroth Legendre moment of the radiative intensity, defined as [4]

$$G(\eta) \equiv 2\pi\int_{\mu=-1}^{1} I(\eta, \mu)\,d\mu, \quad \eta \in [-1, 1]. \tag{2.1b}$$

* The work presented here was supported under grants provided by the Department of Energy (DE-FG05-92ER25138 and DE-FG05-93ER25173).

0021-9991/95 $6.00

Here $I(\eta, \mu)$ is the radiation intensity, $K(\alpha|\eta - \xi|)$ is the kernel which is explicitly given as

$$K(\alpha|\eta - \xi|) = E_1(\alpha|\eta - \xi|), \tag{2.1c}$$

where the exponential integral function is given as [11, p. 228]

$$E_n(z) = \int_{t=0}^{1} t^{n-2} e^{-(z/t)}\, dt, \quad n > 0, \tag{2.1d}$$

and where η is the optical variable and μ is the cosine of the angle between the positive η-direction and the direction of the beam. The optical thickness and single scattering albedo are denoted by L and ω, respectively. Here the two real parameters seen in Eq. (2.1a) are expressible in terms of the single scattering albedo and optical thickness as $\alpha = L/2$ and $\lambda = \omega\alpha$. The forcing function, $f^{\alpha}(\eta)$ contains the imposed boundary constraints in terms of surface intensities and/or internal sources. For purpose of demonstration, we will consider a classical problem (similar to the slab albedo problem in neutron transport), where numerous citations exist. Thus, we will assume that no internal sources are present and that transparent surfaces are present at both $\eta = -1$ and $\eta = 1$. Further, we assume that the front surface at $\eta = -1$ is irradiated by an externally symmetric source while the back surface at $\eta = 1$ is free of any external source. Thus, the forcing function reduces to the nonsingular form

$$f^{\alpha}(\eta) = 2\pi E_2(\alpha(1 + \eta)), \quad \eta \in [-1, 1]. \tag{2.2}$$

Equation (2.1a) represents a linear, weakly singular Fredholm integral equation of the second kind. The weakly singular kernel displayed in Eq. (2.1c) is quadratically integrable [12] in the square $\eta \in [-1, 1]$ and $\xi \in [-1, 1]$, and it is also symmetric. Purely numeric solutions [13, 14] and approximate analytic solutions [15–22] have been presented in the literature. Analytic approaches have typically been based on expansion methods. Legendre polynomials [18, 19] and simple monomials [20–22] have been popular choices for the basis function.

2.2. *Physical Quantities*

Following the notation of Thynell and Ozisik [5] and Frankel [4], we can define two important surface properties. Using the definitions presented in [4], one can express the refectivity, R, as

$$R = \frac{\lambda}{2\pi} \int_{\eta=-1}^{1} G(\eta) E_2(\alpha(1 + \eta))\, d\eta \tag{2.3}$$

and transmissivity, T, as

$$T = 2E_3(2\alpha) + \frac{\lambda}{2\pi} \int_{\eta=-1}^{1} G(\eta) E_2(\alpha(1 - \eta))\, d\eta. \tag{2.4}$$

These properties (and/or exiting surface heat fluxes) are often used as the sole basis for demonstrating accuracy.

3. ANALYSIS

Traditional expansion methods for solving the integral form of the transport equation have used Legendre polynomials [18, 19] and monomials [20–22] as the basis functions. Spiga and his coworkers [23–26] developed numerical solutions using a Galerkin methodology, which is a projection method, for solving an integral form of the one-dimensional transport equation in the presence of different types of scattering phase functions. It should be remarked that projection methods include orthogonal collocation, Ritz–Galerkin, weighted-Galerkin, and least-squares methods. Both Chebyshev polynomials of the first kind [24] and Legendre polynomials of the first kind [23, 25, 26] were used as the basis functions in their expansions. Unfortunately, neither rigorous error estimates nor the theoretical establishment of the convergence rate were presented. The authors remarked that good rates of convergence were established based on numerical evidence. It should also be noted that Kamiuto [27] developed a Chebyshev collocation solution for the spherical harmonics approximation. Again, no error or convergence analysis was provided. In the present work, a general projection framework is established using the residual function from which a particular projection method can be derived.

3.1. *Chebyshev Expansions*

Assume that our real-valued function $G(\eta)$ can be expressed in the form

$$G(\eta) = \sum_{m=0}^{\infty} a_m^* T_m(\eta), \quad \eta \in [-1, 1], \tag{3.1}$$

where $\{T_m(\eta)\}_{m=0}^{\infty}$ are the Chebyshev polynomials of the first kind [28] and follow several well-known relations [11]. The Chebyshev polynomials are defined as

$$T_m(\eta) = \cos[m(\cos^{-1}\eta)], \quad m = 0, 1, \ldots,$$

where $|T_m(\eta)| \leq 1$ for $m \geq 0$. Here the coefficients $\{a_m^*\}_{m=0}^{\infty}$ are to be determined by some practical means. It is well known [28, 29] that $\{T_m(\eta)\}_{m=0}^{\infty}$ form an orthogonal sequence of functions with respect to the weight function $\sqrt{1 - \eta^2}$. Thus, when implementing an expansion method, the main goal lies in determining the unknown expansion coefficients $\{a_m^*\}_{m=0}^{\infty}$. Chebyshev polynomials have several exploitable features [11, 28, 29] and have been the topic of much research and interest with regard to spectral methods [30], boundary value problems [31], nonsingular integral equations [32], and the solution of Cauchy singular integral and integrodifferential equations [33–40].

In general, we seek an approximate solution to $G(\eta)$ by

truncating the infinite series displayed in Eq. (3.1) at a certain order N, namely

$$G_N(\eta) = \sum_{m=0}^{N} a_m^N T_m(\eta), \quad \eta \in [-1, 1], \tag{3.2}$$

where a_m^N is an approximation to a_m^* for each fixed m. Thus, we may express Eq. (2.1a) as

$$R_N(\eta) = G_N(\eta) - f^\alpha(\eta) - \frac{\lambda}{2}\int_{\xi=-1}^{1} E_1(\alpha|\eta - \xi|)G_N(\xi)\, d\xi, \tag{3.3}$$
$$\eta \in [-1, 1], \quad \lambda > 0, \quad \alpha > 0,$$

where we have introduced the local residual function, $R_N(\eta)$. Unless the true solution is a linear combination of $\{T_m(\eta)\}_{m=0}^N$, we cannot choose $\{a_m^N\}_{m=0}^N$ to make $R_N(\eta)$ vanish for all $\eta \in [-1, 1]$. However, suitable expansion coefficients can be obtained by making the residual $R_N(\eta)$ small in some sense.

Let us define the inner product of two real functions $g_1(t)$ and $g_2(t)$ as

$$\langle g_1, g_2\rangle_{w_k} \equiv \int_{t=-1}^{1} w_k(t) g_1(t) g_2(t)\, dt, \tag{3.4a}$$

and the corresponding norm as

$$\|g_1\|_{w_k} = \sqrt{\int_{t=-1}^{1} w_k(t) g_1^2(t)\, dt}, \tag{3.4b}$$

where $w_k(t)$ is a non-negative, real, and integrable weight function.

A particular expansion method is defined by any restrictions imposed on the residual function displayed in Eq. (3.3). Our aim is to determine the unknown expansion coefficients $\{a_m^N\}_{m=0}^N$ in such a manner that some measure of $R_N(\eta)$ is small. A systematic way of expressing this is to require that the orthogonality condition

$$\langle R_N(\eta), \Psi_k(\eta)\rangle_{w_k} = 0, \quad k = 0, 1, ..., N, \tag{3.5}$$

be enforced for $k = 0, 1, ..., N$. In other words, we will require that the residual $R_N(\eta)$ be orthogonal to the first $(N + 1)$ $\Psi_k(\eta)$ functions with respect to the weight function $w_k(\eta)$.

Let the local error in the approximation be defined as

$$\mathscr{E}_N(\eta) = G(\eta) - G_N(\eta), \tag{3.6}$$

and its size may be measured by means of some functional norm. Unfortunately, the error is as inaccessible as the exact solution. However, the residual $R_N(\eta)$ is a computable measure of how well $G_N(\eta)$ is to $G(\eta)$. One can develop a corresponding weakly singular Fredholm integral equation of the second kind for the error $\mathscr{E}_N(\eta)$ in terms of the residual $R_N(\eta)$, namely

$$R_N(\eta) = -\mathscr{E}_N(\eta) + \frac{\lambda}{2}\int_{\xi=-1}^{1} K(\alpha|\eta - \xi|)\mathscr{E}_N(\xi)\, d\xi, \tag{3.7}$$
$$\eta \in [-1, 1].$$

Defining the pth functional norm of $R_N(\eta)$ as $\|R_N\|_p$, and the pth operator norm of $\mathscr{K}$ as $\|\mathscr{K}\|_p$ then one may derive in symbolic form the rigorous error bound [37]

$$\frac{\|R_N\|_p}{1 + (\lambda/2)\|\mathscr{K}\|_p} \le \|\mathscr{E}_N\|_p \le \frac{\|R_N\|_p}{1 - (\lambda/2)\|\mathscr{K}\|_p}, \tag{3.8}$$

(when $1 - (\lambda/2)\|\mathscr{K}\|_p > 0$). Note that $\mathscr{K}$ denotes an integral operator, such as defined by

$$\mathscr{K}g = \int_{\xi=-1}^{1} K(\eta, \xi) g(\xi)\, d\xi,$$

where $K(\eta, \xi)$ is the kernel and g represents some unknown function. This estimate will be discussed further in the next section. It should be noted that we can obtain an analytic expression for the residual, $R_N(\eta)$.

Substituting Eq. (3.2) into Eq. (3.3) yields

$$R_N(\eta) = \sum_{m=0}^{N} a_m^N \left[T_m(\eta) - \frac{\lambda}{2} I_m^\alpha(\eta)\right] - f^\alpha(\eta), \tag{3.9a}$$
$$\eta \in [-1, 1], \quad \lambda > 0,$$

where

$$I_m^\alpha(\eta) = \int_{\xi=-1}^{1} E_1(\alpha|\eta - \xi|) T_m(\xi)\, d\xi, \tag{3.9b}$$
$$m = 0, 1, ..., N, \quad \alpha > 0$$

or, explicitly,

$$I_m^\alpha(\eta) = 2\sum_{j=0}^{[m/2]} \frac{E_{2+2j}(0) T_m^{(2j)}(\eta)}{\alpha^{2j+1}} + \sum_{j=0}^{m} \frac{(-1)^{j+1} E_{j+2}(\alpha(1 + \eta)) T_m^{(j)}(-1)}{\alpha^{j+1}} - \sum_{j=0}^{m} \frac{E_{j+2}(\alpha(1 - \eta)) T_m^{(j)}(1)}{\alpha^{j+1}}, \tag{3.9c}$$
$$m = 0, 1, ..., N, \quad \alpha > 0,$$

where $[m/2]$ denotes the integer resultant. Here, we denote the kth spatial derivative on the mth Chebyshev polynomial as $T_m^{(k)}(\eta)$.

Three methods for determining the expansion coefficients $\{a_m^N\}_{m=0}^N$ are developed in accordance to the concept displayed in Eq. (3.5). The three proposed methods use the weight and

TABLE I

Weights and Test Functions for the Three Expansion Methods

$w_k(\eta)$	$\Psi_k(\eta)$	Name of method
$\delta(\eta - \eta_k)$	1	Collocation
1	$T_k(\eta)$	Ritz-Galerkin
$(1 - \eta^2)^{-1/2}$	$T_k(\eta)$	Weighted-Galerkin

test functions indicated in Table I. Formally proceeding and requiring $\langle R_N, \Psi_k \rangle_{w_k} = 0$ for $k = 0, 1, ..., N$, we arrive at the general expression

$$0 = \sum_{m=0}^{N} a_m^N \int_{\eta=-1}^{1} w_k(\eta)\Psi_k(\eta)\left[T_m(\eta) - \frac{\lambda}{2} I_m^\alpha(\eta)\right] d\eta - \int_{\eta=-1}^{1} w_k(\eta)\Psi_k(\eta) f^\alpha(\eta)\, d\eta, \quad k = 0, 1, ..., N, \quad \lambda > 0, \quad \alpha > 0. \tag{3.10}$$

This equation will be made use of throughout the present analysis.

3.2. *Collocation*

Referring to Table I, the corresponding collocation method requires that $w_k(\eta) = \delta(\eta - \eta_k)$ and $\Psi_k(\eta) = 1$. This implies that the residual $R_N(\eta)$ be zero at $(N + 1)$ discrete collocation points defined by η_k. Thus, we arrive at

$$\sum_{m=0}^{N} a_m^N \left[T_m(\eta_k) - \frac{\lambda}{2} I_m^\alpha(\eta_k)\right] = f^\alpha(\eta_k), \quad k = 0, 1, ..., N, \quad \lambda > 0, \tag{3.11}$$

where $I_m^\alpha(\eta)$ is defined in Eq. (3.9c). This provides $(N + 1)$ equations for determining $(N + 1)$ unknown expansion coefficients. This approach is clearly simple to implement and computationally inexpensive in terms of operation count.

3.3. *Ritz-Galerkin*

Referring to Table I and using $w_k(\eta) = 1$, $\Psi_k(\eta) = T_k(\eta)$, and requiring that $\langle R_N, \Psi_k \rangle_{w_k} = 0$ for $k = 0, 1, ..., N$, we arrive at

$$\sum_{m=0}^{N} a_m^N \left(A_{mk} - \frac{\lambda}{2} C_{mk}^\alpha\right) = f_k^\alpha, \quad k = 0, 1, ..., N, \tag{3.12a}$$

where

$$A_{mk} = \int_{\eta=-1}^{1} T_m(\eta)T_k(\eta)\, d\eta, \quad m = 0, 1, ..., N, \quad k = 0, 1, ..., N, \tag{3.12b}$$

$$C_{mk}^\alpha = \int_{\eta=-1}^{1} I_m^\alpha(\eta)T_k(\eta)\, d\eta, \quad m = 0, 1, ..., N, \quad k = 0, 1, ..., N, \tag{3.12c}$$

$$f_k^\alpha = \int_{\eta=-1}^{1} f^\alpha(\eta)T_k(\eta)\, d\eta, \quad k = 0, 1, ..., N. \tag{3.12d}$$

Explicit expressions for these constants have been derived and can be found in Appendix A. Thus, we are left with a system of $(N + 1)$ linear equations for the $(N + 1)$ unknown expansion coefficients.

3.4. *Weighted-Galerkin*

Some discussion is warranted with regard to this approach. At first glance, it appears that several insurmountable obstacles are present owing to the appearance of the singular weight function displayed in Table I. We can quickly overcome these apparent impediments by expressing the exponential integral function $E_1(\alpha|\eta - \xi|)$ in terms of its standard series representation [11],

$$E_1(\alpha|\eta - \xi|) = -\log|\eta - \xi| - \sum_{j=0}^{\infty} b_j^\alpha |\eta - \xi|^j, \tag{3.13a}$$

where

$$b_0^\alpha = \gamma + \log(\alpha), \tag{3.13b}$$

$$b_j^\alpha = \frac{(-1)^j \alpha^j}{j(j!)}, \quad j = 1, 2, ..., \tag{3.13c}$$

where γ is Euler's constant. We now express Eq. (3.9a) in the explicit form

$$R_N(\eta) = \sum_{m=0}^{N} a_m^N \left[T_m(\eta) + \frac{\lambda}{2}\int_{\xi=-1}^{1} T_m(\xi)\log|\eta - \xi|\, d\xi + \frac{\lambda}{2}\sum_{j=0}^{\infty} b_j^\alpha \int_{\xi=-1}^{1} |\eta - \xi|^j T_m(\xi)\, d\xi\right] - f^\alpha(\eta), \quad \eta \in [-1, 1]. \tag{3.14}$$

Forming the inner product in accordance to Eq. (3.5), we formally arrive at

$$\sum_{m=0}^{N} a_m^N \left[N_{mn} + \frac{\lambda}{2}(A_{mn}\beta_n + B_{mn}^\alpha)\right] = 2\pi\nu_n^\alpha N_{nn}, \quad n = 0, 1, ..., N, \quad \lambda > 0, \tag{3.15}$$

where A_{mn} is defined in Eq. (3.12b) and

$$B^{\alpha}_{mn} = \sum_{j=0}^{\infty} b_j^{\alpha} \int_{\eta=-1}^{1} \frac{T_n(\eta)}{\sqrt{1-\eta^2}} \int_{\xi=-1}^{1} |\eta - \xi|^j T_m(\xi)\, d\xi\, d\eta, \quad \alpha > 0. \tag{3.16}$$

In deriving Eq. (3.15), we made use of the following well-known orthogonality condition associated with Chebyshev polynomials of the first kind, namely [28]

$$N_{mn} = \int_{\eta=-1}^{1} \frac{T_m(\eta)T_n(\eta)}{\sqrt{1-\eta^2}}\, d\eta = \begin{cases} 0, & m \neq n, \\ \pi, & m = n = 0, \\ \dfrac{\pi}{2}, & m = n > 0, \end{cases} \tag{3.17}$$

where N_{mn} is the normalization integral. Additionally, we made use of

$$\int_{\eta=-1}^{1} \frac{T_k(\eta) \log|\eta - \xi|}{\sqrt{1-\eta^2}}\, d\eta = \beta_k T_k(\xi), \tag{3.18a}$$

where

$$\beta_0 = -\pi \log 2, \quad k = 0, \tag{3.18b}$$

$$\beta_k = \pi/k, \quad k > 0. \tag{3.18c}$$

Equation (3.18a) can be derived from [11, 38]

$$⨍_{\eta=-1}^{1} \frac{T_k(\eta)}{\sqrt{1-\eta^2}(\eta - \xi)}\, d\eta = \begin{cases} \pi U_{k-1}(\xi), & k > 0, \\ 0, & k = 0, \end{cases} \tag{3.19}$$

where $U_{k-1}(\xi)$ is the $(k-1)$th Chebyshev polynomial of the second kind [28]. Here ⨍ represents integration in the Cauchy principal value sense [39, 40].

In arriving at Eq. (3.15), we expanded the forcing function $f^{\alpha}(\eta)$ in terms of a Chebyshev series expansion, namely

$$f^{\alpha}(\eta) = 2\pi E_2(\alpha(1+\eta)) = 2\pi \sum_{j=0}^{\infty} \nu_j^{\alpha} T_j(\eta). \tag{3.20}$$

This series representation converges fairly rapidly. In Appendix B, we develop the procedure for determining the expansion coefficients, ν_j^{α}, $j = 0, 1, \ldots$.

Symbolic computation was called upon to integrate, in an exact fashion, the double integral displayed in Eq. (3.16) for B^{α}_{mn}, $m = 0, 1, \ldots, N$; $n = 0, 1, \ldots, N$. Manually, this intermediate level computation is rather tedious. Again, we are now in a position of determining the expansion coefficients from a well-behaved system of linear equations.

4. RESULTS

In this section, we highlight some findings concerning the nature of the Chebyshev polynomials of the first kind and make some comparisons with previously reported results. The rationale for choosing Chebyshev polynomials of the first kind as the basis functions are twofold, namely (i) to develop some new theoretical results and (ii) to extend the results of Kamiuto's results [27] to the integral form of the transport equation. It should be noted that Kamiuto presented only operational results and did not discuss convergence or error estimates in his development of the solution for the integro-differential form of the transport equation.

The two parameter (ω, $L \to \lambda$, α) problem posed here has been previously considered by Lii and Ozisik [41]. The symbolic computation software package Mathematica™, implemented on a NeXT Turbostation with 16 Mbytes of memory, was used for developing the solutions and graphics (with exception to Fig. 2) presented here.

Using Eqs. (2.3) and (2.4) for R, T, respectively, and the finite Chebyshev series representation for $G(\eta)$ displayed in Eq. (3.2), we find

$$R = -\frac{\lambda}{2\pi} \sum_{m=0}^{N} a_m^N \sum_{n=0}^{m} \frac{1}{\alpha^{n+1}} [T_m^{(n)}(1)E_{n+3}(2\alpha) - T_m^{(n)}(-1)E_{n+3}(0)] \tag{4.1}$$

and

$$T = 2E_3(2\alpha) + \frac{\lambda}{2\pi} \sum_{m=0}^{N} a_m^N \sum_{n=0}^{m} \frac{(-1)^n}{\alpha^{n+1}} [T_m^{(n)}(1)E_{n+3}(0) - T_m^{(n)}(-1)E_{n+3}(2\alpha)]. \tag{4.2}$$

It is interesting to note that most studies merely compare R and T results to indicate accuracy. In light of this, we illustrate the effectiveness of the simple collocation method previously described using the Chebyshev polynomials of the first kind. Table II indicates that the collocation approach produces acceptable numerical results for R and T when compared with the exact solution [1, 41] over a range of optical thicknesses and single-scattering albedos. The collocation points were established from a closed, Gauss-Chebyshev (Lobatto-Chebyshev) [9] rule, i.e., $\eta_k = \cos(\pi k/N)$, $k = 0, 1, \ldots, N$. This closed rule ensures that $R_N(1) = R_N(-1) = 0$.

Lii and Ozisik [41] also included exact and approximate results when the optical thickness, L was 15 and 30 for the cases where the single-scatter albedo approached unity. The orthogonal collocation method outlined here proved to produce excellent numerical results when compared to the exact results reported in [41]. For example, when $\omega = 0.995$, $L = 15$ and $L = 30$, the exact results for the reflectivity and transmissivity

TABLE II

Comparison of the Present Collocation Results for R and T to the Exact Results [41] for Various Optical Thicknessess, L, and Albedos, ω

ω	Surface property	$L = 0.5$ ($N = 7$)		$L = 1$ ($N = 7$)		$L = 2$ ($N = 9$)		$L = 5$ ($N = 11$)	
		Present	Exact	Present	Exact	Present	Exact	Present	Exact
0.995	R	0.2932	0.2932	0.4412	0.4412	0.5988	0.5988	0.7636	0.7636
	T	0.7018	0.7018	0.5488	0.5488	0.3815	0.3815	0.1892	0.1892
0.9	R	0.2475	0.2475	0.3527	0.3527	0.4372	0.4376	0.4764	0.4763
	T	0.6599	0.6599	0.4747	0.4747	0.2656	0.2656	0.0534	0.0534
0.8	R	0.2056	0.2056	0.2802	0.2806	0.3280	0.3280	0.3417	0.3417
	T	0.6220	0.6220	0.4162	0.4162	0.1973	0.1973	0.0229	0.0229
0.7	R	0.1690	0.1690	0.2221	0.2221	0.2506	0.2506	0.2566	0.2565
	T	0.5891	0.5891	0.3712	0.3712	0.1551	0.1551	0.0124	0.0124
0.6	R	0.1365	0.1365	0.1743	0.1743	0.1919	0.1919	0.1948	0.1947
	T	0.5603	0.5603	0.3356	0.3355	0.1269	0.1269	0.0077	0.0077
0.5	R	0.1077	0.1077	0.1342	0.1342	0.1451	0.1451	0.1466	0.1465
	T	0.5350	0.5350	0.3067	0.3067	0.1071	0.1071	0.0053	0.0053
0.3	R	0.0584	0.0584	0.0701	0.0701	0.0741	0.0741	0.0745	0.0745
	T	0.4924	0.4925	0.2631	0.2631	0.0814	0.0814	0.0030	0.0030
0.1	R	0.0178	0.0178	0.0208	0.0207	0.0216	0.0216	0.0217	0.0217
	T	0.4580	0.4578	0.2319	0.2317	0.0659	0.0658	0.0021	0.0020

were reported [41] as $R = 0.8438$, $T = 0.0450$ and $R = 0.8497$, $T = 0.0071$, respectively. Correspondingly, Lii and Ozisik [41] reported that their approximate solution produced $R = 0.8429$, $T = 0.0453$ and $R = 0.8489$, $T = 0.0070$, respectively. The orthogonal collocation method embodied here for the case $L = 15$, $\omega = 0.995$ produced $R = 0.843896$, $T = 0.044943$ (when $N = 13$) and $R = 0.843853$, $T = 0.044956$ (when $N = 15$). When $L = 30$, $\omega = 0.995$, the present method produced $R = 0.850151$, $T = 0.007036$ (when $N = 13$), $R = 0.849919$, $T = 0.0070495$ (when $N = 15$), and $R = 0.849816$, $T = 0.0070556$ (when $N = 17$). Clearly, the exact solution is supportive of these representative results. At various other albedos, it has been shown that accurate numerical results are obtained. Additionally, no numerical instabilities emerged from the computations required in arriving at any results reported in this paper.

When $\omega = 1$, Lii and Ozisik [41] did not report any results for the reflectivity and transmissivity and thus no basis of comparison can be made with that study. However, the present methodology has provided accurate results when $\omega = 1$ as verified by rigorous error estimates and by physical trends (i.e., $\omega \to 1$) without any special modification to the analytic procedure or computer code.

Being an exploratory investigation, some additional characteristics associated with the approximation should be elucidated. Some additional theoretic considerations can be developed from knowledge of the residual function, $R_N(\eta)$. As remarked earlier, an analytic expression for $R_N(\eta)$ can be developed, namely

$$R_N(\eta) = -f^{\alpha}(\eta) + \sum_{m=0}^{N} a_m^N \Bigg[T_m(\eta) - \frac{\lambda}{2} \Bigg\{ 2 \sum_{j=0}^{[m/2]} \frac{E_{2+2j}(0) T_m^{(2j)}(\eta)}{\alpha^{2j+1}} + \sum_{j=0}^{m} \frac{(-1)^{j+1} E_{j+2}(\alpha(1+\eta)) T_m^{(j)}(-1)}{\alpha^{j+1}} - \sum_{j=0}^{m} \frac{E_{j+2}(\alpha(1-\eta)) T_m^{(j)}(1)}{\alpha^{j+1}} \Bigg\} \Bigg], \quad \eta \in [-1, 1], \quad \alpha > 0, \quad \lambda > 0, \tag{4.3}$$

which is valid for the three methods previously discussed.

Some clarification concerning the weighted-Galerkin method must be made here. In order to perform all the integrations analytically, the forcing function $f^{\alpha}(\eta)$, which contained the exponential integral function, $E_2(\alpha(1 + \eta))$, was expanded into an equivalent Chebyshev series (see Appendix B). Thus, the forcing function was approximated to some extent. Appendix B contains some details on the errors associated with this approximation. The Ritz–Galerkin method did not suffer a similar fate since the integration involving the forcing function, weight function, and coordinate function could be performed without approximation.

Figure 1 (a–d) present $G_N(\eta)$ and $R_N(\eta)$ for the three discussed methods (b-collocation, c-Ritz–Galerkin, d-weighted-Galerkin), where $N = 7$, $\alpha = 1$, and $\lambda = 0.8$. In Fig. 1b, the collocation points were chosen in accordance to $\eta_k =$

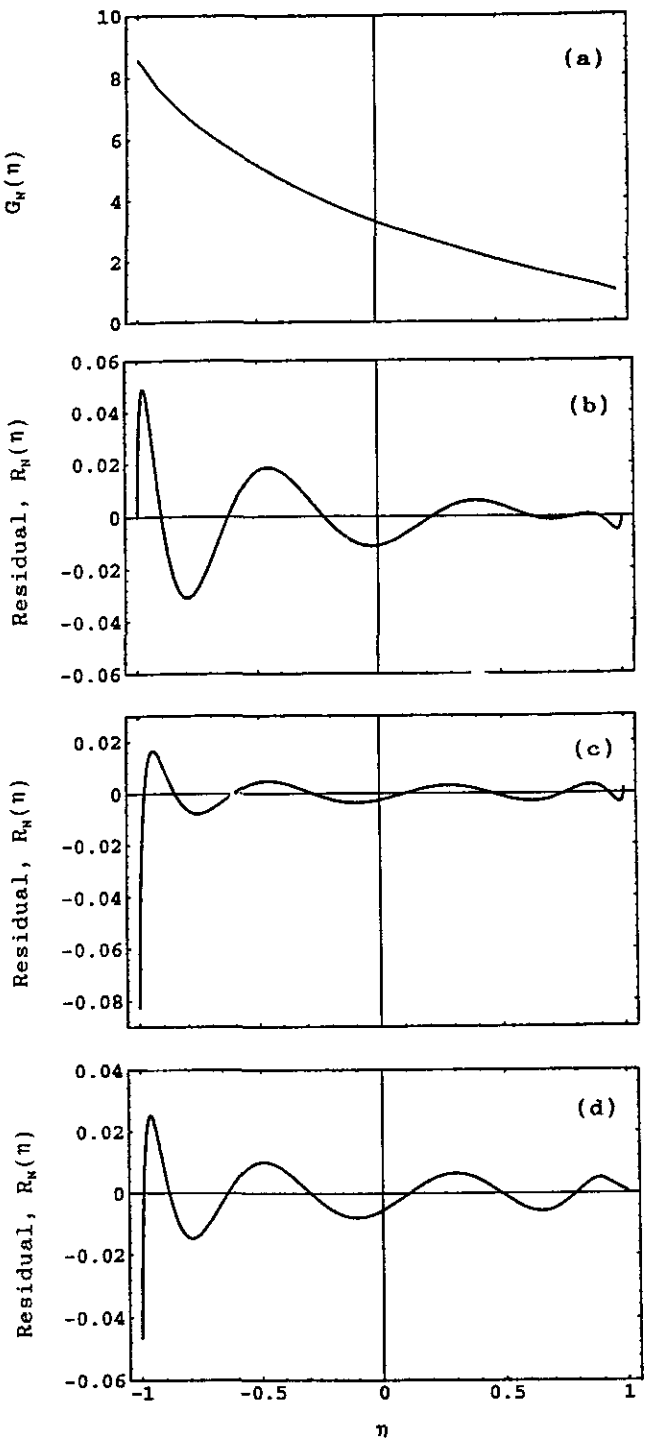

FIG. 1. The approximate solution, $G_N(\eta)$, and residual plots, $R_N(\eta)$, for the methods of: (b) collocation; (c) Ritz-Galerkin; and (d) weighted-Galerkin, where $N = 7$, $\omega = 0.8$, $L = 2$ ($\lambda = 0.8$, $\alpha = 1$).

$\cos(k\pi/N)$, $k = 0, 1, ..., N$. The oscillatory characteristic associated with the residual are somewhat similar to each other with the exception of the obvious enforcement of $R_N(1) = R_N(-1) = 0$ by the collocation method. The effect of the Chebyshev weight function is also evident when comparing the Ritz- and weighted-Galerkin methods near $\eta = -1$ and $\eta = 1$. These approaches produced graphically identical $G_N(\eta)$ results as displayed in Fig. 1a. Observe that the approximate solution $G_N(\eta)$ is bounded while the kernel shown in Eq. (2.1c) is not.

It is clear from viewing Fig. 1b that the residuals for the orthogonal collocation method at the endpoints are zero as forced by construction using the collocation points defined by a closed rule. Some numerical methods have indicated that large errors take place at the endpoints in $G(\eta)$. However, the orthogonal collocation method offered here (and also clearly demonstrated by Frankel [42]) illustrates that excellent numerical results can be achieved at these locations. Clearly, the residual plots offer some insight into this phenomenon.

From the residual plots, the collocation method appears to produce comparable results to that of the Galerkin methods. Realizing the extensive amount of arithmetic associated with Galerkin methods due to multiple integrals, it appears that the collocation method represents an economical and accurate Nth-order approximation to $G(\eta)$. Computer times for calculating the expansion coefficients for the orthogonal collocation, Ritz–Galerkin, and weighted-Galerkin methods when $N = 6$ were 18 s, 48 s, and 3380 s, respectively. It should be remarked that the individually prepared codes where not optimized for speed. The last approach is clearly excessive, owing to the numerous analytic manipulations required as described in Appendix B. The numerical implementation offered by Spiga and Spiga [24] appears to be advantageous over the present weighted-Galerkin method in terms of speed although no quantitative run times were reported in [24]. Doubling N approximately squares the CPU time required for calculating the expansion coefficients. Most of the CPU time used in a single run for small N was attributed to calculating the norms of the various functions and kernels required in arriving at rigorous error estimates.

Total memory requirements for a complete simulation which involves the determination of the expansion coefficients, reconstruction of the solution, and other important physical parameters, error analysis, and graphical outputs for the collocation method when $N = 6$ was 1.28 Mbytes while for $N = 12$ the memory requirement was 2.03 Mbytes. Clearly these requirements are reasonable. Increasing N for the collocation method does not require excessive amounts of memory. The Galerkin methods require additional memory of approximately 1 Mbyte. These requirements are rather flexible, since they depend on how one writes the computer code.

As alluded to earlier, the unknown expansion coefficients $\{a_m^N\}_{m=0}^N$ are found by solving a system of coupled linear algebraic equations by matrix means. Owing to the obvious coupling among the coefficients, the effect of N on the accuracy of a_m^N must also be considered. Table III illustrates the effect of the number of terms retained in the collocation expansion on the convergence of the expansion coefficients when $\alpha = 1$ and $\lambda = 0.8$. Clearly, the dominant terms are converging as N grows.

With regard to Tables IV and V, both the Ritz–Galerkin

TABLE III

Convergence of the Collocation Expansion Coefficients when $\omega = 0.8$, $L = 2$ ($\lambda = 0.8$, $\alpha = 1$)

a_i^N	$N = 3$	$N = 5$	$N = 7$	$N = 9$	$N = 11$	$N = 13$
a_0^N	4.00079	3.97947	3.97582	3.97469	3.97424	3.97402
a_1^N	−3.58873	−3.50197	−3.49091	−3.48776	−3.48652	−3.48593
a_2^N	0.823741	0.732223	0.722387	0.719784	0.718793	0.718333
a_3^N	−2.242179	−0.257857	−0.239203	−0.235060	−0.233589	−0.232929
a_4^N		0.0976552	0.0774224	0.073513	0.0722306	0.0716811
a_5^N		−0.0490953	−0.0575897	−0.0505265	−0.0484691	−0.0476382
a_6^N			0.0318984	0.0245541	0.0226228	0.0218904
a_7^N			−0.0185276	−0.0233762	−0.0200245	−0.0188587
a_8^N				0.0145546	0.0112132	0.0101349
a_9^N				−0.00890106	−0.0118907	−0.0100779
a_{10}^N					0.0078602	0.00611486
a_{11}^N					−0.00493661	−0.00690141
a_{12}^N						0.00472646
a_{13}^N						−0.00301481
R	0.332869	0.328332	0.328015	0.327968	0.327957	0.327954
T	0.195848	0.197152	0.197253	0.197266	0.197268	0.197269
$\|\mathscr{E}_N\|_\infty^U$	0.668451	0.283302	0.153469	0.0954606	0.0648849	0.0468881
$\|\mathscr{E}_N\|_\infty^L$	0.126754	0.0537207	0.0291013	0.0181016	0.0123037	0.0088911

and weighted-Galerkin methods produce similar convergence trends on the expansion coefficients as compared with the collocation method. Tables III through V also present the resulting numerical values for the reflectivity R and transmissivity T using a finite Chebyshev series representation for the unknown function, $G(\eta)$. From viewing Tables III through V, it is clear that as N grows, accurate numerical results for these two surface properties are being generated. From Table II, the exact values corresponding to Tables III–V for R and T are 0.03280 and 0.01973, respectively. It appears that four places of accuracy can be quickly obtained for both R and T, even though the expansion coefficients have not converged to a comparable number of places for small N. Some care should be exercised when using $G_N(\eta)$ when N is small.

At this point, it is instructive to define the infinity norm of a function as

TABLE IV

Convergence of the Ritz-Galerkin Expansion Coefficients when $\omega = 0.8$, $L = 2$ ($\lambda = 0.8$, $\alpha = 1$)

	$N = 3$	$N = 5$	$N = 7$	$N = 9$
a_0^N	3.95562	3.96844	3.97149	3.97259
a_1^N	−3.46102	−3.47630	−3.48095	−3.48267
a_2^N	0.677921	0.706724	0.713145	0.715377
a_3^N	−0.204947	−0.222733	−0.227756	−0.229558
a_4^N		0.0584488	0.0661107	0.0685639
a_5^N		−0.0359049	−0.0420111	−0.0440163
a_6^N			0.0154309	0.0184535
a_7^N			−0.0122815	−0.0147768
a_8^N				0.00607399
a_9^N				−0.00501322
R	0.3278841	0.3279440	0.3279493	0.3279502
T	0.1972424	0.1972684	0.1972696	0.1972697
$\|\mathscr{E}_N\|_\infty^U$	0.960897	0.44594	0.258666	0.171938
$\|\mathscr{E}_N\|_\infty^L$	0.182209	0.0845608	0.0490492	0.0326035

TABLE V

Convergence of the Weighted-Galerkin Expansion Coefficients when $\omega = 0.8$, $L = 2$ ($\lambda = 0.8$, $\alpha = 1$)

	$N = 3$	$N = 5$	$N = 7$	$N = 9$
a_0^N	3.97928	3.97458	3.97395	3.97379
a_1^N	−3.48853	−3.48579	−3.48529	−3.48514
a_2^N	0.728443	0.718416	0.717832	0.717713
a_3^N	−0.236790	−0.232418	−0.232099	−0.232027
a_4^N		0.0725636	0.0710985	0.0709772
a_5^N		−0.0476729	−0.0466972	−0.0466069
a_6^N			0.0214933	0.0210767
a_7^N			−0.0179622	−0.0176301
a_8^N				0.00924411
a_9^N				−0.00861693
R	0.329405	0.328196	0.328024	0.327979
T	0.197923	0.197342	0.197286	0.197275
$\|\mathscr{E}_N\|_\infty^U$	0.591802	0.259727	0.145653	0.092896
$\|\mathscr{E}_N\|_\infty^L$	0.112222	0.0492504	0.0276193	0.0176153

TABLE VI
Error Bounds (L_∞-norm) for the Collocation Method when $\omega = 0.8$, $L = 2$ ($\lambda = 0.8$, $\alpha = 1$)

N	$\|\mathscr{E}_N\|_\infty^L$	$\|\mathscr{E}_N\|_\infty^n$	$\|\mathscr{E}_N\|_\infty^U$
1	0.5373	2.17	2.834
2	0.2513	0.71	1.325
3	0.1268	0.28	0.6685
4	0.08079	0.16	0.4261
5	0.05372	0.0987	0.2833
6	0.0391	0.069	0.2063
7	0.02913	0.051	0.1535
8	0.02280	0.039	0.1202
9	0.01810		0.09546
10	0.01486		0.07835
11	0.01230		0.06489
12	0.01043		0.05498
13	0.008891		0.04689

$$\|\Theta\|_\infty \equiv \operatorname*{Sup}_{\eta\in[-1,1]} |\Theta(\eta)|. \tag{4.5a}$$

Correspondingly, the infinity norm of the integral operator $\mathscr{K}$ is [7, p. 14]

$$\|\mathscr{K}\|_\infty \equiv \operatorname*{Sup}_{\eta\in[-1,1]} \int_{\xi=-1}^{1} |K(\alpha|\eta-\xi|)|\, d\xi, \tag{4.5b}$$

and where the infinity norm of the residual function becomes

$$\|R_N\|_\infty \equiv \operatorname*{Sup}_{\eta\in[-1,1]} |R_N(\eta)|. \tag{4.5c}$$

Observe that, for this physical problem, the Galerkin methods produce their extremal at $\eta = -1$, unlike the collocation method where the extremal of $R_N(\eta)$ is located in the interior of the physical domain. Thus, when calculating the L_∞-norm of the residual for the collocation method, some additional numerical/symbolic analysis is performed in order to locate the corresponding extremal.

A rigorous L_∞-error bound $\|\mathscr{E}_N\|_\infty$ for $G_N(\eta)$ is available from Eq. (3.8). For the three methods, the error bounds are also presented in Tables III through V. The upper-error bound has the superscript U while the lower-error bound has the superscript L. It is clear from viewing Tables III through V that there is more error in $G_N(\eta)$ for fixed N than is realized in either R or T.

For comparison purposes, a simple numeric solution for solving the weakly singular Fredholm integral equation for the local error $\mathscr{E}_N(\eta)$, shown in Eq. (3.7), has been carried out using the residual generated by the collocation method when $\alpha = 1$ and $\lambda = 0.8$. Table VI presents the discrete L_∞-error as obtained by direct numerical simulation for this illustrative case. These numerical results were obtained by solving the weakly singular Fredholm integral equation of the second kind shown in Eq. (3.7), using singularity subtraction and trapezoidal integration [4]. Here, the numerically obtained L_∞ norm of $\mathscr{E}_N(\eta)$ denoted by $\|\mathscr{E}_N\|_\infty^n$ (superscripted with an "n" for numerical) is contrasted to the upper and lower bounds as developed by Eq. (3.8). It is interesting to note that the error tends toward the lower bound for this case rather rapidly. Using the results shown in column 4 for the numerically obtained L_∞-error from the integral equation, we can extract useful information concerning the convergence rate of the method. The convergence rate associated with a solution method is a crucial factor in determining the success of the method. The information presented in Table VI permits empirical interpretation toward estimating the convergence rate. Examination of column 3 in Table VI circumstantially indicates that the convergence rate can be approximated by the expression

$$\|\mathscr{E}_N\| \approx \|\mathscr{E}_N\|_\infty^n = O(1/N^2), \tag{4.6}$$

where N is the order of the expansion. In Appendix C, a pessimistic estimate is developed based on a projection method [7, 34, 40, 41]. This approach produces

$$\|\mathscr{E}_N\|_\infty = O(\ln(N)/N^r), \tag{4.7}$$

where $G \in C^r[-1, 1]$ Note that our observational skill relied on fairly low values of N, while the estimate developed in Appendix C required N sufficiently large (greater than our observational data). In general, a viable expansion technique should have rapid convergence.

Finally, Table VII demonstrates the influence of the parameters L, ω on the upper and lower L_∞-error bounds as the number of terms in the Chebyshev series is increased. As the optical thickness increases and the single-scattering albedo decreases, the bounds appear to be tightening (although apparently large in magnitude) rapidly as N increases.

5. CONCLUSIONS

Several expansion methods have been implemented for solving the equation of radiative transfer in an isotropically scattering, absorbing, and potentially emitting media, using Chebyshev polynomials of the first kind as the basis functions. The practical analytical/computational procedure offered here was assisted by the implementation of symbolic computation in determining the expansion coefficients. Symbolic manipulation was effective in assisting the development of some of the error analysis presentation within. The collocation technique using this choice of basis augmented by symbolic computation offers an easy and obvious generalization to situations involving anisotropic scatter [4, 5] and spatially varying albedos [22, 43] in both plane-parallel and spherical geometries [43]. The rate of convergence for the series representation offered by the orthogonal collocation method is deemed moderate. The collocation method appears especially noteworthy with regard to flexability

TABLE VII

Error Bounds (L_∞-norm) for Several Optical Thicknesses, L, and Albedos, ω

N	L	ω	$\|\mathscr{E}_N\|_\infty^L$	$\|\mathscr{E}_N\|_\infty^U$
5	0.1	0.8	0.00530256	0.00699654
	1	0.8	0.0317676	0.105959
	10	0.8	0.186451	1.67066
5	0.1	0.2	0.00981479	0.0105148
	1	0.2	0.088425	0.115948
	10	0.2	0.786421	1.17914
7	0.1	0.8	0.00279293	0.00368517
	1	0.8	0.0169058	0.056388
	10	0.8	0.111123	0.995692
7	0.1	0.2	0.00505042	0.00541063
	1	0.2	0.0456048	0.0597997
	10	0.2	0.414734	0.621843
9	0.1	0.8	0.0025158	0.00331951
	1	0.8	0.0104246	0.0347706
	10	0.8	0.0734615	0.658237
9	0.1	0.2	0.00410602	0.00439887
	1	0.2	0.0277234	0.0363525
	10	0.2	0.254447	0.381513

as noted by Frankel [44] when investigating transient, radiative-conductive transport in a participating medium.

LaClair and Frankel [45] extended the present work to include a linear anisotropic scattering phase function. Novel error estimates were also obtained extending the procedure offered here to two coupled, weakly singular, Fredholm integral equations of the second kind. Again, symbolic computation was called upon for performing numerous and often tedious analytic manipulations. Numerical studies investigating combined-mode heat transfer using a generalization of the method of Kumar and Sloan [45] as demonstrated in [44], and highly anisotropic radiative transport, such as in coal-fired combustion [47], are tractable via collocation.

In closing, the accuracy of a numerical method for the radiative equation of transfer based on R and T comparisons should be carefully examined. In many practical applications, the actual spatial distribution of the intensity or the zeroth (or first) moment of the intensity appear crucial, owing to coupling to another dependent variable such as temperature. A clear error estimate (or bounds) on the unknown function(s) certainly serves to permit a proper evaluation of accuracy.

APPENDIX A

Explicit expressions for the constants displayed in Eqs. (3.12b)–(3.12d) are

$$A_{mk} = \begin{cases} 0, & m, k \text{ mixed odd/even}, \\ \dfrac{1}{1-(m+k)^2} + \dfrac{1}{1-|m-k|^2}, & \text{both } m, k \text{ even or odd}, \end{cases} \tag{A.1}$$

and

$$\begin{aligned} C_{mk}^{\alpha} = {} & 2\sum_{j=0}^{M} \frac{E_{2+2j}(0)}{\alpha^{2j+1}} \int_{\eta=-1}^{1} T_k(\eta) T_m^{(2j)}(\eta)\, d\eta + \sum_{j=0}^{m} \frac{1}{\alpha^{j+1}} \\ & \left\{ (-1)^j T_m^{(j)}(-1) \sum_{n=0}^{k} \frac{1}{\alpha^{n+1}} [T_k^{(n)}(1) E_{n+j+3}(2\alpha) \right. \\ & - T_k^{(n)}(-1) E_{n+j+3}(0)] - T_m^{(j)}(1) \sum_{n=0}^{k} \frac{(-1)^n}{\alpha^{n+1}} [T_k^{(n)}(1) E_{n+j+3}(0) \\ & \left. - T_k^{(n)}(-1) E_{n+j+3}(2\alpha)] \right\}, \end{aligned} \tag{A.2}$$

where $M = \text{int}[m/2]$ and where the integral term is expressible as

$$\begin{aligned} \int_{\eta=-1}^{1} T_k(\eta) T_m^{(2j)}(\eta)\, d\eta &= \sum_{n=0}^{m-2j} c_{jknm} \int_{\eta=-1}^{1} T_k(\eta) T_n(\eta)\, d\eta \\ &= \sum_{n=0}^{m-2j} c_{jknm} A_{nk} \end{aligned} \tag{A.3}$$

for evaluation purposes. Symbolic software packages such as Mathematica™ or Maple permit the rapid evaluation of the constants c_{jknm} as needed when expressing $T_m^{(2j)}(\eta)$ in terms of a finite Chebyshev sum. Maple has a function already prepared for doing this operation. This tedious procedure can be done by hand by initiating the process [28]

$$\begin{aligned} T_m^{(1)}(\eta) &= mU_{m-1}(\eta) \\ &= \begin{cases} m\left[1 + 2\sum_{j=2,4,..}^{m-1\geq 2} T_j(\eta)\right], & m \text{ odd}, \\ m\left[2\sum_{j=1,3,..}^{m-1\geq 1} T_j(\eta)\right], & m \text{ even}, \end{cases} \\ T_m^{(2)}(\eta) &= \begin{cases} 2m\left[\sum_{j=2,4,..}^{m-1\geq 2} (2j) \sum_{k=1,3,..}^{j-1\geq 1} T_k(\eta)\right], & m \text{ odd}, \\ 2m\left[\sum_{j=1,3,..}^{m-1\geq 1} (2j)\left[\frac{1}{2} + \sum_{k=2,4,..}^{j-1\geq 2} T_k(\eta)\right]\right], & m \text{ even}, \end{cases} \end{aligned}$$

$$T_m^{(3)}(\eta) = \begin{cases} 2m\left[\sum_{j=2,4,\ldots}^{m-1\geq 2}(2j)\sum_{k=1,3,\ldots}^{j-1\geq 1}(2k)\left[\frac{1}{2}+\sum_{n=2,4,\ldots}^{k-1\geq 2}T_n(\eta)\right]\right], & m \text{ odd}, \\ 2m\left[\sum_{j=1,3,\ldots}^{m-1\geq 1}(2j)\sum_{k=2,4,\ldots}^{j-1\geq 2}(2k)\sum_{n=1,3,\ldots}^{k-1\geq 1}T_n(\eta)\right], & m \text{ even}, \end{cases}$$

....

$m = 0, 1, \ldots$, where $U_n(\eta)$ is the nth Chebyshev polynomial of the second kind [28]. Clearly, a pattern is developing but symbolic manipulation appears to be more prudent and better suited to such computation than the author. Finally,

$$f_k^\alpha = -2\pi\sum_{n=0}^{k}\frac{1}{\alpha^{n+1}}[E_{3+n}(2\alpha)T_k^{(n)}(1) - E_{3+n}(0)T_k^{(n)}(-1)], \quad k = 0, 1, \ldots. \tag{A.4}$$

APPENDIX B

In this appendix, we briefly describe the approximation of the second exponential integral function in terms of a Chebyshev series representation. Consider [11]

$$E_2(\alpha(1+\eta)) = \alpha(1+\eta)\ln(1+\eta) - \sum_{k=0}^{\infty}\beta_k^\alpha(1+\eta)^k, \quad \eta\in[-1,1], \tag{B.1}$$

where

$$\beta_0^\alpha = -1$$
$$\beta_1^\alpha = \alpha(1-\gamma-\ln(\alpha))$$
$$\beta_k^\alpha = \frac{(-\alpha)^k}{(k-1)k!}, \quad k>1.$$

Assuming that $E_2(\alpha(1+\eta))$ can be expressed as

$$E_2(\alpha(1+\eta)) = \sum_{m=0}^{\infty}\nu_m^\alpha T_m(\eta), \quad \eta\in[-1,1], \tag{B.2a}$$

where

$$\nu_m^\alpha = \frac{1}{N_{mm}}\int_{\eta=-1}^{1}\frac{E_2(\alpha(1+\eta))t_m(\eta)}{\sqrt{1-\eta^2}}d\eta, \quad m = 0, 1, \ldots, \tag{B.2b}$$

where the normalization integral, N_{mn} is defined in Eq. (3.17). Making use of [28]

TABLE VIII

Relative Error of $E_2(\alpha(1+\eta))$ as a Function of the Terms Retained in the Finite Chebyshev Expansion ($\alpha = 1$)

η	$\lvert\delta_7\rvert$	$\lvert\delta_9\rvert$	$\lvert\delta_{11}\rvert$
−1	1.78971	1.11111	0.757576
−0.8	1.02045	0.302367	0.230138
−0.6	0.395868	0.48912	0.301628
−0.4	1.23546	0.721127	0.229382
−0.2	1.0343	0.229182	0.05697277
0	1.79653	0.873624	0.486842
0.2	1.4602	1.12263	0.746734
0.4	2.77448	1.91536	0.613317
0.6	2.73703	1.74141	0.30272
0.8	2.16854	2.46278	0.563874
1.0	4.24428	3.03923	1.74353

$$T_m(\eta)T_k(\eta) = \tfrac{1}{2}[T_{m+k}(\eta) + T_{|m-k|}(\eta)] \tag{B.3}$$

and noting that [38, p. 218]

$$h_k(\eta) = \int_{\xi=1}^{1}\frac{T_k(\xi)\ln|\eta-\xi|}{\sqrt{1-\xi^2}}d\xi = \begin{cases} -\pi\ln(2), & k=0, \\ -\dfrac{\pi T_k(\eta)}{k}, & k\geq 1, \end{cases} \tag{B.4}$$

we arrive at

$$\nu_m^\alpha N_{mm} = -\sum_{k=0}^{\infty}\beta_k^\alpha\int_{\eta=-1}^{1}\frac{T_m(\eta)(1+\eta)^k}{\sqrt{1-\eta^2}}d\eta + \frac{\alpha}{2}[2h_m(-1) + h_{m+1}(-1) + h_{|m-1|}(-1)], \quad m = 0, 1, \ldots. \tag{B.5}$$

The evaluation of the remaining integral in (B.5) for each fixed m is performed analytically with the aid of Mathematica™.

Table VIII presents the relative error, as defined by

$$|\delta_N| = \left|\frac{E_2(\alpha(1+\eta)) - \sum_{n=0}^{N}\nu_n^\alpha T_n(\eta)}{E_2(\alpha(1+\eta))}\right| \times 100.$$

Clearly, even at $N = 11$ (i.e., with 12 terms in the series representation) a fair amount of error persists. Thus, it appears that a direct numerical approximation for

$$\int_{\eta=-1}^{1}\frac{f^\alpha(\eta)T_k(\eta)}{\sqrt{1-\eta^2}}d\eta, \quad k = 0, 1, \ldots, N,$$

is preferable.

APPENDIX C

A brief discussion concerning the rate of convergence associated with the approximate solution based on the collocation method using the closed-rule collocation points previously described is now presented. The results obtained in this appendix are intended to clarify the observed convergence rate conjectured by Eq. (4.6). Our approach relies on the projection method framework described by Atkinson [7], Baker [48], and others [38]. We refer the reader to these fine sources for the particulars.

Let $G \in C^r[-1, 1]$, $N > r$, and let the points $\eta_k \in [-1, 1]$ be given by $\eta_k = \cos[k\pi/N]$, $k = 0, 1, ..., N$. Define the interpolatory projection operator P_N such that

$$P_N h = \sum_{m=0}^{N} l_m(\eta) h(\eta_m), \tag{C.1a}$$

where $h(\eta)$ is a real function such that $h \in C^r[-1, 1]$ and where $l_m(\eta)$ is the Lagrange interpolation polynomial [49, 50]

$$l_m(\eta) = \prod_{k=0(\neq m)}^{N} \frac{(\eta - \eta_k)}{(\eta_m - \eta_k)}, \quad m = 0, 1, ..., N. \tag{C.1b}$$

For implementation purposes, we express Eq. (C.1b) as

$$l_m(\eta) = \frac{\Omega(\eta)}{\Omega'(\eta_m)(\eta - \eta_m)}, \quad \eta \in [-1, 1], \tag{C.1c}$$

where

$$\Omega(\eta) = \prod_{k=0}^{N} (\eta - \eta_k), \tag{C.1d}$$

$$\Omega'(\eta_m) = \prod_{k=0(\neq m)}^{N} (\eta_m - \eta_k). \tag{C.1e}$$

Let us also define s_N such that it is a polynomial of degree $\leq N$. The linear operator P_N has the property [7]

$$P_N s_N = s_N, \tag{C.2a}$$

from which we can derive the idempotent property [7]

$$P_N^2 = P_N; \tag{C.2b}$$

also note that $\|P_N\|_\infty \geq 1$ for $N \geq 1$. Let the previously defined collocation points also represent the interpolatory points. Also, note that η_k, $k = 0, 1, ..., N$, are real, distinct, and symmetric around $\eta = 0$. For large N, the points are more dense around the endpoints than toward the center of the interval $\eta \in [-1, 1]$. With this in mind, it is clear from its construction that

$$P_N \mathrm{R}_N(\eta) = \sum_{k=0}^{N} R_N(\eta_k) l_k(\eta) = 0 \tag{C.3a}$$

and

$$P_N R_N(\eta_m) = \sum_{k=0}^{N} R_N(\eta_k) l_k(\eta_m) = \sum_{k=0}^{N} R_N(\eta_k)\, \delta_{mk} = 0, \tag{C.3b}$$

where δ_{mk} is the Kronecker delta function and $R_N(\eta)$ is the local residual function defined in Eq. (3.3) and explicitly expressed in Eq. (4.3). Recall that Eq. (3.3) and Eq. (2.1a), respectively, in their corresponding operator form as

$$R_N = G_N - f^\alpha - \frac{\lambda}{2} \mathcal{K} G_N, \tag{C.4a}$$

$$0 = G - f^\alpha - \frac{\lambda}{2} \mathcal{K} G, \tag{C.4b}$$

where we assume that $\lambda/2$ is a regular value of $\mathcal{K}$. Operating on Eqs. (C.4a–C.4b) with P_N and noting that G_N is a polynomial of degree N, we find that

$$0 = G_N - P_N f^\alpha - \frac{\lambda}{2} P_N \mathcal{K} G_N, \tag{C.5a}$$

$$0 = P_N G - P_N f^\alpha - \frac{\lambda}{2} P_N \mathcal{K} G. \tag{C.5b}$$

Adding and subtracting G from Eq. (C.5b) and then taking the difference between Eqs. (C.5a) and (C.5b) yields

$$\left(I - \frac{\lambda}{2} P_N \mathcal{K}\right)(G - G_N) = G - P_N G,$$

or

$$G - G_N = \left(I - \frac{\lambda}{2} P_N \mathcal{K}\right)^{-1} (G - P_N G), \tag{C.6}$$

where

$$\lim_{N \to \infty} \|P_N \mathcal{K} - \mathcal{K}\|_\infty = 0$$

than for sufficiently large N, $(I - (\lambda/2) P_N \mathcal{K})^{-1}$ exists [7]. Taking the infinity norm of Eq. (C.6) produces

$$\|G - G_N\|_\infty = \left\| \left(I - \frac{\lambda}{2} P_N \mathcal{K}\right)^{-1} (G - P_N G) \right\|_\infty,$$

or

$$\|G - G_N\|_\infty \leq \frac{1}{1 - (\lambda/2)\|P_N \mathcal{K}\|_\infty} \|G - P_N G\|_\infty. \tag{C.7}$$

Introducing the best uniform approximation [40] γ_N (a polynomial of degree $\leq N$), we find that

$$\|G - G_N\|_\infty \leq \frac{1}{1 - (\lambda/2)\|P_N\mathcal{H}\|_\infty} \|(G - \gamma_N + \gamma_N - P_N G)\|_\infty.$$

but, since $\gamma_N = P_N\gamma_N$, we find that

$$\|G - G_N\|_\infty = O[(1 + \|P_N\|_\infty)\|G - \gamma_N\|_\infty]. \qquad (C.9)$$

From Baker [48, p. 93], one can show that

$$\|G - \gamma_N\|_\infty = O(1/N^r).$$

These results came about from the use of a Jackson theorem [48]. Before proceeding, a digression is warranted.

Rivlin [49] and others have investigated a case similar to the present study, except that they considered an open-rule set of Chebyshev collocation points. The values of $\|P_N\|_\infty^x$ for $N > 0$ with collocations points defined by $\eta_j^x = \cos[(2j - 1)\pi/2N], j = 1, ..., N$, has been analytically developed in several sources [48, 49]. Rivlin [49, pp. 93–97] showed that

$$\Lambda_N^x = \sum_{m=1}^{N} |l_m(\eta)| < \frac{2}{\pi}\ln(N) + 4, \qquad (C.10a)$$

where Λ_N^x is the Lebesgue constant which has at most logarithmic growth. Conforming to our notation, let

$$\|P_N\|_\infty^x = \frac{2}{\pi}\ln(N) + 4. \qquad (C.10b)$$

Rivlin [49, p. 93] remarks that the proof of this result is "rather long." In fact, Baker [48, p. 94] adds that this result is "pessimistic." Baker [48, p. 94] further remarks that for $N < 1000$, $\Lambda_N^x < 5.4$. (Note that a typographical error exists in his result for Λ_N^x on p. 94.) Baker [48, p. 104] does indicate that the closed-rule collocation points should produce a similar relation as indicated in Eq. (C. 10a) although the constants involved would be different.

Owing to the numerous applications of the triangle inequality, an empirical approach for bounding $\|P_N\|_\infty$ appears quite reasonable. With these remarks in mind, a contemporary approach representing a compromise between theory and practice is offered with the aid of symbolic manipulation. One can empirically demonstrate, to a high degree of confidence and accuracy, that

$$\|P_N\|_\infty = A\ln(N) + B, \qquad (C.11)$$

for sufficiently large N. This is graphically demonstrated in Fig. 2. The approximate numerical values for A and B agree well with Ref. [28, p. 13]. Figure 2 presents a semilog graph which indicates a straightline for sufficiently large N. Numerical results for this figure were generated using the definition of $\|P_N\|_\infty$ based on Eqs. (C.1c)–(C.1e) and implemented using Mathematica™.

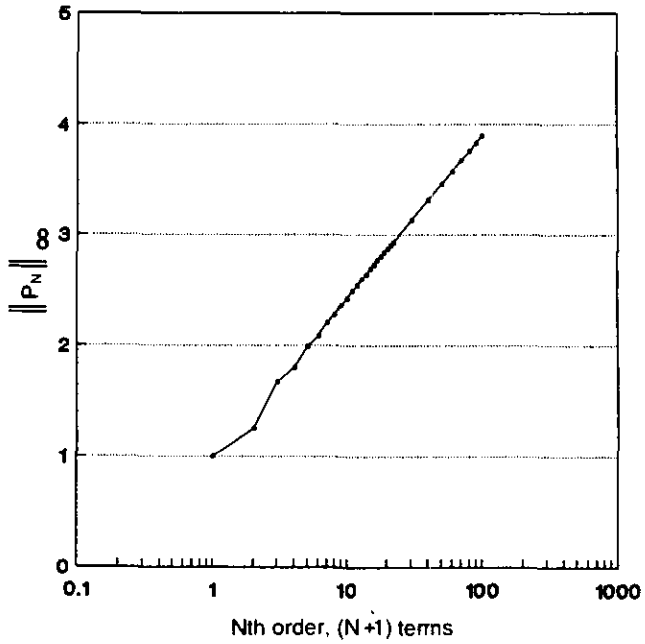

FIG. 2. Symbolically calculated relation indicating functional dependence of $\|P_N\|_\infty$ on N with interpolatory points defined by $\eta_k = \cos[k\pi/N]$, $k = 0, 1, ..., N$.

Thus, it appears that from our theoretical development that

$$\|\mathcal{E}_N\|_\infty = \|G - G_N\|_\infty = O(\ln(N)/N^r). \qquad (C.12)$$

These results indicate that rapid convergence will occur if $G(\eta)$ is sufficiently smooth. This result appears to have direct bearing on regularity of the unknown function $G(\eta)$. The reported discrepency between Eq. (C.12) and Eq. (4.6) could come about due to (i) the conjecture for extracting Eq. (4.6) is based on $N < 9$ (not sufficiently large) and (ii) Eq. (C.12) is a pessimistic result due to the bounding processes involved.

In the general anisotropic case, or in situations involving mixed-mode, nonlinear heat transfer, this type of analysis appears quite formidable although in some cases it does appear possible.

REFERENCES

1. M. N. Ozisik, *Radiative Transfer* (Wiley, New York, 1980).
2. V. C. Boffi and G. Spiga, *J. Math. Phys.* **18,** 2448 (1977).
3. J. J. Duderstadt and W. R. Martin, *Transport Theory* (Wiley, New York, 1979).
4. J. I. Frankel, *Quant. Spectrosc. Radiat. Transfer* **46,** 329 (1991).

5. S. T. Thynell and M. N. Ozisik, *J. Appl. Phys.* **60,** 541 (1986).
6. A. Kisomi and W. H. Sutton, *J. Thermophys. Heat Transfer* **2,** 370 (1988).
7. K. E. Atkinson, *A Survey of Numerical Methods for the Solution of Fredholm Integral Equations of the Second Kind Solution of Fredholm Integral Equations of the Second Kind* (SIAM, Philadelphia, 1976).
8. A. L. Crosbie and M. Pattabongse, *Quant. Spectrosc. Radiat. Transfer* **34,** 473 (1985).
9. L. M. Delves and J. L. Mohamed, *Computational Methods for Integral Equations* (Cambridge Univ. Press, Cambridge, 1988).
10. K. E. Atkinson, *Numerical Analysis* (Wiley, New York, 1989).
11. M. Abramowitz and I. A. Stegun (Eds.), *Handbook of Mathematical Functions* (Dover, New York, 1965).
12. H. Kschwendt, *J. Comput. Phys.* **5,** 84 (1970).
13. A. Sharma and A. C. Cogley, *Numer. Heat Transfer* **5,** 21 (1982).
14. H. Khalil, J. K. Shultis, and T. J. Lester, *Numer. Heat Transfer* **5,** 235 (1982).
15. N. J. McCormick and M. R. Mendelson, *Nucl. Sci. Engrg.* **20,** 462 (1964).
16. W. H. Sutton and M. N. Ozisik, *Quant. Spectrosc. Radiat. Transfer* **22,** 55 (1979).
17. M. S. Abdel Krim, *Astrophys. Space Sci.* **164,** 69 (1990).
18. Y. A. Cengel and M. N. Ozisik, *Quant. Spectrosc. Radiat. Transfer* **32,** 225 (1984).
19. Y. A. Cengel and M. N. Ozisik, ASME Paper 86-HT-28, Boston, MA, 1986 (unpublished).
20. M. N. Ozisik and Y. Yener, *J. Heat Transfer* **104,** 351 (1982).
21. Y. A. Cengel, M. N. Ozisik, and Y. Yener, *J. Heat Transfer* **106,** 248 (1984).
22. Y. A. Cengel, M. N. Ozisik, and Y. Yener, *Int. J. Heat Mass Transfer* **27,** 1919 (1984).
23. G. Spiga, F. Santarelli, and C. Stramigioli, *Int. J. Heat Mass Transfer* **23,** 841 (1980).
24. G. Spiga and M. Spiga, *Ann. Nucl. Energy* **12,** 307 (1985).
25. G. Spiga and M. Spiga, *Int. Commun. Heat Mass Transfer* **10,** 191 (1983).
26. F. Santarelli, C. Stramigioli, and G. Spiga, *Int. J. Heat Mass Transfer* **23,** 853 (1980).
27. K. Kamiuto, *Quant. Spectrosc. Radiat. Transfer* **35,** 329 (1986).
28. T. J. Rivlin, *The Chebyshev Polynomials* (Wiley, New York, 1974).
29. C. K. Lu, *J. Math. Anal. Appl.* **100,** 416 (1984).
30. S. A. Orszag, *J. Fluid Mech.* **50,** 689 (1971).
31. A. Zehbib, *J. Comput. Phys.* **53,** 443 (1984).
32. R. Piessens, and M. Branders, *J. Comput. Phys.* **21,** 178 (1976).
33. N. I. Ioakimidis, *Math. Comput.* **41,** 79 (1983).
34. F. Erdogan, *SIAM J. Appl. Math.* **17,** 1041 (1969).
35. J. I. Frankel, *Q. Appl. Math.*, in press.
36. J. I. Frankel (unpublished).
37. I. Barrodale, in *Numerical Solution of Integral Equations*, edited by L. M. Delves and J. Walsh (Oxford Univ. Press, London, 1974), p. 101.
38. M. A. Golberg, in *Numerical Solution of Integral Equations*, edited by M. A. Golberg (Plenum, New York, 1990), p. 183.
39. F. G. Tricoma, *Integral Equations* (Dover, New York, 1985).
40. N. I. Muskhelishvili, *Singular Integral Equations*, 2nd ed. (Dover, New York, 1992).
41. C. C. Lii and M. N. Ozisik, *Int. J. Heat Mass Transfer* **16,** 685 (1973).
42. J. I. Frankel, in *Boundary Element Technology IX*, edited by C. A. Brebbia and A. J. Kassab (Comput. Mech. Publ., Southampton, 1994), p. 51.
43. S. T. Thynell and M. N. Ozisik, *J. Heat Transfer* **107,** 732 (1985).
44. J. I. Frankel, *AIAA J. Thermophys. Heat Transfer*, to appear.
45. T. LaClair and J. I. Frankel, *Int. J. Numer. Methods Heat Fluid Flow*, in press.
46. S. Kumar and I. H. Sloan, *Math. Comput.* **48,** 585 (1987).
47. M. P. Menguc and R. Viskanta, *Quant. Spectrosc. Radiat. Transfer* **29,** 381 (1983).
48. C. T. H. Baker, *The Numerical Treatment of Integral Equations* (Clarendon Press, Oxford, 1978).
49. T. J. Rivlin, *An Introduction to the Approximation of Functions* (Blaisdell, London, 1969).
50. E. W. Cheney, *Introduction to Approximation Theory* (McGraw–Hill, New York, 1966).